DOI:
10.1093/carcin/bgac102

Document Version
Peer reviewed version

NamiRNA-enhancer network of miR-492 activates the NR2C1-TGF-β/Smad3 pathway to promote epithelial-mesenchymal transition of pancreatic cancer

Shanshan Liu[1, #], Xiaomeng He[1, #], Yang Di[2, #], Qiuyue Li[1, #], Feng Li[1, #], Yan Ma[1], Litian Chen[3], Yushi Gao[1,4], Jingjing Xu[1], Shuai Yang[5], Li Xu[1], Christopher Corpe[6], Yun Ling[1], Xiaoyan Zhang[1], Jianqing Xu[1], Wenqiang Yu[1,5], Jin Wang[1, *]

[1]Shanghai Public Health Clinical Center, Fudan University, Shanghai, China; [2]Department of Pancreatic Surgery, Huashan Hospital, Fudan University, Shanghai, China; [3]Department of Hepatobiliary Surgery, Shanghai Jiaotong University School of Medicine Xinhua Hospital, Shanghai, China; [4]School of Life Sciences, Hubei University, Wuhan, 430062, China; [5]Institutes of Biomedical Sciences, Shanghai Medical College, Fudan University, Shanghai, China; [6]King's College London, London, Nutritional Science Department, 150 Stamford Street, Waterloo, London, SE19NH, United Kingdom.

The authors declare no potential conflicts of interest.

*Correspondence should be addressed to:

Jin Wang, M.D. & Ph.D.

Scientific Research Center,

Shanghai Public Health Clinical Center

Fudan University

2901 Caolang Road, Jinshan District

Shanghai 201508, China

Ph: 86-21-57036495

Fax: 86-21-57247094

Email: wjincityu@yahoo.com

[#] These authors contributed equally to this work.

Abstract

Pancreatic cancer (PaCa) is one of the most fatal malignancies of the digestive system, and most patients are diagnosed at advanced stages due to the lack of specific and effective tumor-related biomarkers for the early detection of PaCa. miR-492 has been found to be upregulated in PaCa tumor tissue and may serve as a potential therapeutic target. However, the molecular mechanisms by which miR-492 promotes PaCa tumor growth and progression are unclear. In this study, we first found that miR-492 in enhancer loci activated neighboring genes (NR2C1/NDUFA12/TMCC3) and promoted PaCa cell proliferation, migration, and invasion *in vitro*. We also observed that miR-492-activating genes significantly enriched the TGF-β/Smad3 signaling pathway in PaCa to promote epithelial-mesenchymal transition (EMT) during tumorigenesis and development. Using CRISPR–Cas9 and ChIP assays, we further observed that miR-492 acted as an enhancer trigger, and that antagomiR-492 repressed PaCa tumorigenesis *in vivo*, decreased the expression levels of serum TGF-β, and suppressed the EMT process by downregulating the expression of NR2C1. Our results demonstrate that miR-492, as an enhancer trigger, facilitates PaCa progression *via* the NR2C1-TGF-β/Smad3 pathway.

Keywords: miR-492, pancreatic cancer, NamiRNA, enhancer, EMT, TGF-β/Smad3

Graphical abstract

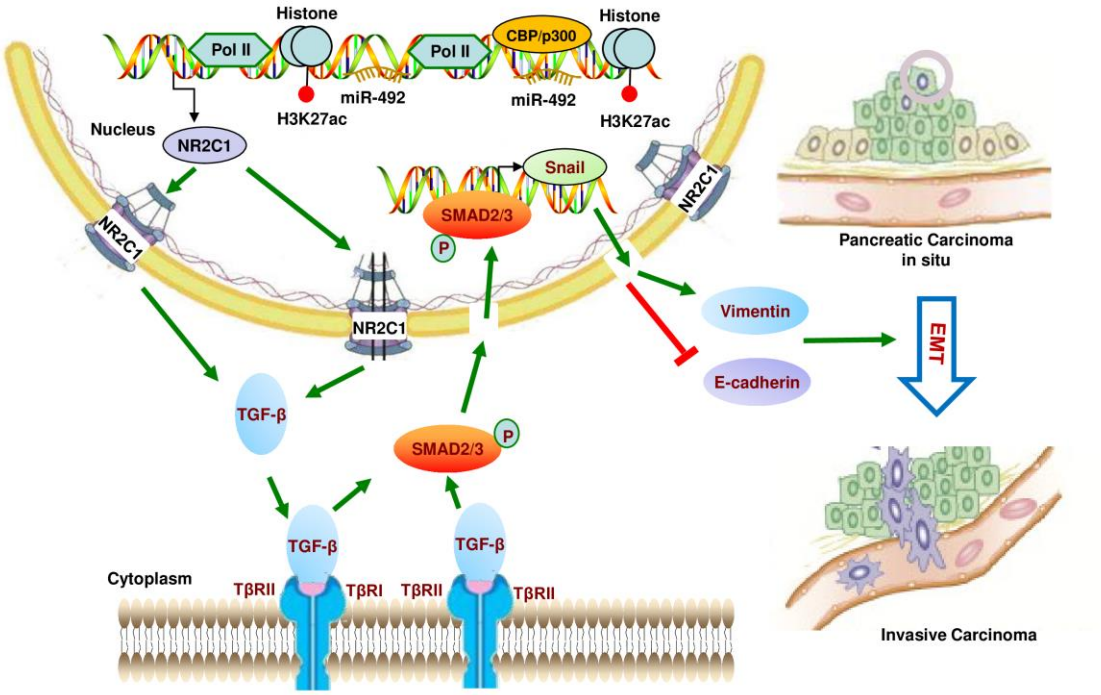

Summary

We found that miR-492 acts as an enhancer trigger to activate the neighboring genes NR2C1/NDUFA12/TMCC3 in pancreatic cancer. miR-492 promotes EMT progression of pancreatic cancer *via* the NR2C1-TGF-β/Smad3 pathway.

Introduction

Pancreatic cancer (PaCa) is a rare malignant tumor of the digestive tract and is one of the most lethal malignancies in the world (1). PaCa patients have a 5-year survival rate of 6.9% (2). Surgical resection is currently the only potentially curative therapy, but most patients are diagnosed at advanced stages due to a lack of specific and effective tumor-related biomarkers and miss their chance for curative treatment (3,4). The epithelial to mesenchymal transition (EMT) is associated with tumor invasion and metastasis in pancreatic cancer, and TGF-β, as a major inducer of EMT during cancer progression, has drawn considerable attention (5). Many aberrantly expressed miRNAs are highly related to disease progression in multiple cancer types and have been identified as tumor biomarkers that modulate tumorigenesis, tumor proliferation, apoptosis and metastasis (6,7). Our previous study demonstrated that differentially expressed miR-492 was present in pancreatic tumor tissue and pancreatic juice from patients with PaCa and was tightly correlated with the prognosis of PaCa patients (8). However, the precise role of miR-492 in PaCa development is unknown.

miR-492 is known to originate from the coding sequence of keratin 19 (KRT19), is most strongly influenced by PLAG1 (pleomorphic adenoma gene 1) in hepatoblastoma (9) and is highly expressed in various tumors, such as bladder cancer, breast cancer, gastric cancer, liver cancer, ovarian cancer, prostate cancer and rectal cancer (9-16). miR-492 can significantly enhance cell proliferation, migration and invasion of hepatoblastoma and breast cancer and is involved in the radiotherapy response of cervical squamous cell carcinomas by directly targeting CD44 (17), SOX7 (10) or TIMP2 (18). Knockdown of miR-492 inhibits cell proliferation and metastasis of bladder cancer and retinoblastoma by targeting gap junction beta-4 protein (GJB4) (13) or large tumor suppressor kinase 2 (LATS2) (19).

Some miRNAs are able to modulate gene expression either by binding to the 3' untranslated regions (3'UTRs) of mRNA (20-22) or by promoting mRNA degradation. In addition, nuclear activating miRNAs (NamiRNAs) can transcriptionally activate gene expression by targeting enhancers (23-26). Multiple duplex RNAs complementary to the progesterone receptor (PR) promoter have been shown to increase the expression of PR protein and reduce the expression of cyclooxygenase-2 (COX-2) (27). Small RNAs complementary to sequences beyond the 3' terminus of PR mRNA can also modulate the expression of PR, induce chromatin changes at the PR promoter, and affect responses to physiological stimuli (28). Some miRNAs have also been identified as enhancer triggers and can activate gene transcription by targeting specific sites of their promoters. It is well known that enhancers are cis-regulatory elements that can exist at long distances from their target genes and regulate their expression. The histone marker H3K27ac has been used to identify and classify enhancer regions and can be detected to distinguish 'active' enhancers from poised enhancers (29). NamiRNAs are enhancer-overlapping miRNAs that function as enhancer triggers (30). For example, miR-339 positively modulates GPER1 as a cis-regulator via an enhancer (30). miR-589 can bind promoter RNA and activate COX-2 transcription (23). miR-24, as an enhancer trigger, activates enhancer RNA expression, alters histone modification, and increases the enrichment of p300 and RNA Pol II (25). miR-205 can specifically activate tumor suppressor genes (IL-4, IL-32) by targeting specific sites in their promoters (24). In this study, we first used the UCSC genome browser and observed that the enhancer marker H3K27ac was enriched in the miR-492 region, where the neighboring genes of miR-492 were NR2C1, NDUFA12 and TMCC3. Together, these data suggest that miR-492 may act as a NamiRNA to activate gene transcription in pancreatic cancer. Thus, the objective of the current study was to investigate the potential involvement of miR-492 in positively regulating the expression levels of neighboring genes. Our data indicate that miR-492, as an enhancer

trigger via the NamiRNA enhancer network, facilitated PaCa progression by affecting the expression levels of its neighboring genes (NR2C1/NDUFA12/TMCC3) and the NR2C1-TGF-β/Smad3 pathway, suggesting that miR-492 has potential as a diagnostic and therapeutic target for PaCa.

Methods and Materials

Tissue sample and RNA extraction

A total of 54 PaCa tissues and paracancerous tissues (> 5 cm away from the PaCa tissues) were collected from the Department of Pancreatic Surgery, Huashan Hospital Affiliated with Fudan University (Shanghai, China). All of the patients were diagnosed with PaCa. Blanket consent for research studies was obtained at the time of surgery from the patients. Total RNA was extracted from the tissues and cells using TRIzol and chloroform reagents following the manufacturer's instructions (Invitrogen, Carlsbad, California, USA).

Cell lines and cell culture

All cell lines were purchased from ATCC (American Type Culture Collection) on Jan. 2019. Human PaCa cell lines (CAPAN-1, CAPAN-2, NOPR1, CFPAC-1, SUIT2, SW1990 and MiaPaCa-2) were cultured in DMEM (Dulbecco's modified Eagle's medium, Thermo Fisher), PANC-1 cells were cultivated in DMEM-F12 (DMEM/Ham's F-12, BBI, China), and BxPC-3, AsPC-1, and KP3 cells were maintained in RPMI-1640 medium supplemented with 10% FBS and 1% penicillin and streptomycin. HPNE was maintained in DMEM (Dulbecco's modified Eagle's medium, Thermo Fisher) supplemented with 10% fetal bovine serum (FBS, Thermo Fisher Scientific, Waltham, MA, US), 1 mg/mL puromycin, 1 μg/μL

epidermal growth factor (EGF) and M3: Base F medium (INCELL Corporation LCC, USA). All cell lines were authenticated prior to their use and tested for mycoplasma contamination every 3 months. All cells were cultured in a humidified atmosphere at 37 °C with 5% CO_2.

Immunohistochemical staining

Immunohistochemical (IHC) staining for NR2C1 (Cat#: YN0089, Immunoway, USA), NDUFA12 (Cat#: YN0919, Immunoway, USA), TMCC3 (Lot#: JC26, Absin, Shanghai, China), rabbit anti-E-cadherin (Cat#: ab15148, Abcam, UK), rabbit anti-vimentin (Cat#: ab137321, Abcam, UK) and rabbit anti-SNAIL+SLUG (Cat#: ab85936, Abcam, UK) was performed in formalin-fixed, paraffin-embedded mouse tumor tissue samples. The stained fields were photographed using a light microscope equipped with a camera (CKX41, Olympus, Japan). The study was approved by Shanghai Public Health Clinical Center institutional review boards.

Chromatin immunoprecipitation (ChIP)

The transfected cells were harvested and crosslinked with 1% formaldehyde for 10 minutes at room temperature. After sonication, the soluble chromatin was incubated with 5 μg of antibody. Chromatin immunocomplexes were then precipitated with Protein A or Protein G magnetic beads. The immunoprecipitated complexes were washed, and DNA was extracted and purified. ChIP DNA was analyzed by qPCR using specific primers, and the data were normalized to input DNA. The results were derived from three independent experiments. The antibodies used were anti-H3K27ac (Cat#: ab4729, Abcam, UK), anti-p300 (Cat#: D161648,

BBI, China), anti-pol Ⅱ (Cat#: 202693-T34, Sino Biological, China) and anti-Argonaute 2 (C34C6, Cell Signaling Technology Inc., Boston, Massachusetts, USA).

Coimmunoprecipitation (Co-IP) assay

Co-IP was performed using the indicated antibodies and IgG according to the manufacturer's instructions. In brief, cells were harvested and lysed directly on plates for 30 min. Then, 50 μL protein A/G (Selleck, China) was incubated with 5 μg H3K27ac antibody (Cat#: ab177178, Abcam, UK) overnight at 4 °C. Then, the protein lysate was mixed with the bead-antibody complex at 4 °C for 2 h. The immunoprecipitants were washed three times, boiled with SDS loading buffer, and subsequently analyzed by immunoblotting with the appropriate antibodies.

Western blots

Cytoplasmic and nuclear extracts were obtained using nuclear and cytoplasmic extraction reagents (BBI, Shanghai, China). For protein isolation from cells, RIPA buffer with proteinase inhibitor was used. The protein concentration was measured using a BCA assay (Beyotime, China). Thirty micrograms of total protein was loaded per lane and separated on a 10% sodium dodecyl sulfate-polyacrylamide gel by electrophoresis, and then the proteins were transferred onto nitrocellulose membranes. The membranes were blocked with 5% milk in PBST and then incubated with rabbit anti-NR2C1 (Cat#: YN0089, Immunoway, USA), rabbit anti-NDUFA12 (NDUAC) (Cat#: YN0919, Immunoway, USA), rabbit anti-TMCC3 (Cat#: abs101863, Absin, Shanghai, China), rabbit anti-E-cadherin (Cat#: ab15148, Abcam, UK), rabbit anti-vimentin (Cat#: ab137321, Abcam, UK), rabbit anti-SNAIL+SLUG (Cat#:

ab85936, Abcam, UK), rabbit anti-lamin A/C (Cat#: 10298-1-AP, Proteintech, USA), rabbit anti-p300 (Cat#: 104491-T10, SinoBiological, China), rabbit anti-pol II (Cat#: 202693-T34, SinoBiological, China), rabbit anti-H3K27ac (Cat#: ab177178, Abcam, UK) or HSP 90 rabbit mAb (C45G5) (Cat#: 4877, Cell Signaling Technology Inc., USA) at 4 °C. After washing with PBST, the blots were treated with a horseradish peroxidase (HRP)-conjugated anti-rabbit IgG antibody for 1 h at room temperature. Finally, the blot was visualized using an enhanced chemiluminescence detection system.

Clustered regularly interspaced short palindromic repeats and associated proteins 9 (CRISPR–Cas 9)-based system of genome editing

Single guide RNAs (sgRNAs) were manually designed, and then synthetic sgRNAs (5'-CACCGAGTGGCTGTAGTTGTGGGA-3'; 5'-AAACTCCCACAACTACAGC CACTC-3'; 5'-ACACCGAGTTTGGTTTGAGTGTTTGG-3'; 5'-AAAACCAAAC ACTCAAACCAAACTCG-3') were inserted into Cas9-based HP180_px300_GFP vectors. HEK293T cells were transfected with Cas9-based HP180_px300_GFP recombinant plasmids. After 48 h, the transfected cells with GFP were sorted into 96-well plates that already contained 200 μL of cell culture medium per well using fluorescence-activated cell sorting (FACS, BD FACSAria II, USA). After two weeks of incubation, genomic DNA was extracted from clones using a TIANamp Blood DNA Kit (TIANGEN Biotech, Cat#: DP304-02, Beijing, China) according to the manufacturer's protocol. Each clone was screened using the same PCR primers (forward primer: GATGAGGGAAATGAGACAGAAAAAGG, reverse primer: CGAGCTGAATCCACCCTCACATG) and T7 Endonuclease I cleavage assay (New England Biolabs, Lot#: 10078800, USA). Then, cleavage products were

identified using DNA agarose electrophoresis. Finally, the positive clones with the desired deletion were selected and moved to larger plates for growth.

Dual luciferase reporter assays

The predicted enhancer region containing the miR-492 locus was inserted into the pGL3-promoter plasmid for enhancer activity assays. Then, the cell extracts were prepared after transfection for 48 hours and assayed using a Dual Luciferase Reporter Assay System (Promega) according to the manufacturer's protocol. Renilla luciferase was used to normalize for transfection efficiency, and the ratio of firefly/Renilla luciferase activities defined the relative activity of the enhancer region.

Xenograft tumor mouse model and bioluminescence imaging analysis

All animal studies were conducted in strict accordance with the guidelines of the Animal Care and Use Committee of the Shanghai Public Health Clinical Center. For the xenograft tumor model, BxPC-3 cells bearing lentivirus-luciferase were cultured and further modified to stably express the luciferase gene by lentivirus transfection to facilitate *in vivo* monitoring of tumor development. These cells were grown to 80% confluence, harvested by 0.25% trypsinization, washed twice with PBS, resuspended to a final concentration of 2 x 10^6 cells/100 μL in PBS, and injected subcutaneously into the right back of 8-week-old BALB/c male nude mice. A week later, the nude mice with subcutaneous BxPC-3 cell tumors were randomly divided into two groups: one group was given tail vein injections of 5 nmol antagomir-492, and a control group was given an equivalent volume of PBS (5 mice in each

group). The weight of the mice was measured every three days. The mice were injected every three days for a total of six times.

Tumor growth was assessed by bioluminescence imaging. Before the mice in each group were imaged, they were given an intraperitoneal injection of D-luciferin. Then, the mice were anesthetized with 1% sodium pentobarbital by intraperitoneal injection, and images were captured after 15 min. The anesthetized mice were placed on the imaging platform of an Ultra-Sensitive Whole Sample Imaging System (NightOWL^{TM}, Berthold, Germany). The analyses of fluorescence were performed in WinLight 32 software (Berthold, Germany). The mice were then sacrificed humanely, and the tumors were harvested for RNA, protein, immunohistochemical (IHC) and HE staining analyses.

Statistical Analysis

Data analyses were performed using the SPSS statistical package 25.0 (SPSS Inc., Chicago, IL, USA). All experiments in this study were performed independently with at least three biological replicates. The data are presented as the means ± standard deviations from three independent experiments and were evaluated using a Student's t tests. $p < 0.05$ was considered statistically significant (* $p < 0.05$, ** $p < 0.01$ and *** $p < 0.001$). Some analyses were also performed using GraphPad Prism 9 software (GraphPad Software, San Diego, CA, USA).

Results

miR-492 acts as a transcriptional activator for neighboring genes in enhancer loci in pancreatic cancer

In this study, we first found by qRT–PCR analysis that the miR-492 expression levels were significantly increased in most PaCa cells compared to normal pancreatic HPNE cells, especially in the AsPC-1, BxPC-3 and CAPAN-2 cell lines (Fig. 1A). We also designed a specific miR-492 probe to detect its intracellular distribution by in situ hybridization, which revealed that miR-492 was mainly distributed in the cytoplasm and nucleus In contrast, U6 snRNA was mainly distributed in the nucleus and miR-16 localized primarily in the cytoplasm (Fig. 1C). We also found that miR-492 was significantly upregulated in PaCa tissues compared with adjacent normal tissues ($p < 0.05$) and that 53.7% (29 of 54) of PaCa tissues showed upregulation of miR-492 compared with the corresponding normal pancreatic tissues (Fig. 1B). To clarify the molecular mechanism of miR-492 in PaCa, we hypothesized that miR-492 regulates its neighboring genes by targeting promoter elements. We next found that H3K27ac modification was abundant in the miR-492 genomic region, and the neighboring genes of miR-492 were NR2C1, NDUFA12 and TMCC3 on chromosome 12 (Fig. 1D). Then, we used qRT–PCR to analyze adjacent gene NR2C1/NDUFA12/TMCC3 expression levels. We found that, compared with the HPNE cell line, the levels of NR2C1 and TMCC3 were highly expressed in PANC-1 cells, and NUDFA12 was also upregulated in the AsPC-1 cell line (Fig. 1E-G). Moreover, NR2C1/NDUFA12/TMCC3 expression levels were significantly increased in 54 fresh PaCa tissues compared with those in the paired corresponding paracancerous tissues ($p < 0.01$; Fig. 1H-J). A total of 72.2% (39 of 54), 64.8% (35 of 54) and 70.3% (38 of 54) of the PaCa tissues showed a more than 2-fold upregulation in NR2C1, NDUFA12 and TMCC3 mRNA expression levels when compared with the corresponding normal pancreatic tissues, respectively. To further analyze the

correlation between NR2C1, NDUFA12 and TMCC3 gene expression levels, we used StarBase 2.0 (https://starbase.sysu.edu.cn/) to analyze the expression levels of three genes in 178 PaCa tumor samples from the TCGA database. Our results showed that TMCC3 was positively correlated with NR2C1 (r = 0.394; $p < 0.001$; Fig. S1A) and NDUFA12 (r = 0.297; $p < 0.001$; Fig. S1B). Similarly, there was a positive correlation between NR2C1 and NDUFA12 gene expression (r = 0.455; $p < 0.001$; Fig. S1C).

To determine whether overexpression of miR-492 was able to enhance neighboring gene expression, we constructed a miR-492 plasmid and obtained reproducible ectopic high-level miRNA expression. As expected, we confirmed that the overexpression of miR-492 in BxPC-3 and PANC-1 cells resulted in concurrent increases in the transcription of neighboring NR2C1, NDUFA12, and TMCC3 genes by 5.2-, 1.7- and 4.5-fold in BxPC-3 cells, respectively (Fig. 1K). Increased RNA levels of NR2C1, NDUFA12, and TMCC3 (136-fold, 8.3-fold and 360-fold, respectively) were also observed in PANC-1 cells overexpressing miR-492 (Fig. 1L). As predicted, the miR-492 precursor can indeed activate its neighboring genes from its loci. To determine whether mature miRNA participated in triggering activation, we also transfected BxPC-3 and PANC-1 cells with miR-492 mimics and observed that the neighboring genes of miR-492 were markedly increased (Fig. 1K and 1L). Our results also showed an increased protein level of NR2C1/NDUFA12/TMCC3 in both BxPC-3 and PANC-1 cells overexpressing miR-492 compared with the control group, as shown by immunoblots (Fig. 1N and 1O), which demonstrated that mature miRNA can also elevate the mRNA levels of its respective neighboring gene, similar to precursor miRNA. To further evaluate miRNA function, miR-492 was silenced by transfecting BxPC-3 and PANC-1 cells with a miR-492 inhibitor. qPCR showed that the suppression of miR-492 notably reduced the mRNA expression levels of NR2C1, NDUFA12 and TMCC3 by 0.34-0.58-, 0.40-0.79-, and 0.45-0.65-fold in BxPC-3 and PANC-1 cells compared with controls (Fig.

1M) and protein levels (Fig. 1N and 1O). A nuclear fraction with high purity was isolated from BxPC-3 and PANC-1 cells. As shown in Fig. 1P and Fig. 1Q, when miR-492 was overexpressed, TMCC3 and NDUFA12 were increased in the cytoplasm, whereas NR2C1 was increased in the nucleus. Immunofluorescence analyses also revealed that NR2C1 was expressed in the nucleus and upregulated when PaCa cells were transfected with premiR-492 (Fig. S2), which indicates that miR-492 might act as an enhancer trigger to activate NR2C1 gene expression in PaCa cells and suggests that miR-492 functions as a NamiRNA (31).

In contrast, miR-331 was chosen as a negative control because it does not possess H3K27ac enhancer activating capacity, although miR-331 is an adjacent miRNA of miR-492 and has neighboring genes (NR2C1, NDUFA12, FGD6 and VEZT; Fig. S3A). We investigated whether the expression levels of NR2C1/NDUFA12/FGD6/VEZT were significantly elevated after the transfection of miR-331 mimics or premiR-331 into BxPC-3 (Fig. S3B) and PANC-1 cells (Fig. S3C). The neighboring genes of miR-331 were also not downregulated by the miR-331 inhibitor (Fig. S3D), which indicates that H3K27ac enrichment is a necessary marker for potential enhancer elements of miR-492 activating its neighboring genes.

miR-492 function as NamiRNA is dependent on the presence of an intact enhancer and altered chromatin state

We first found that the enhancer marker H3K27ac was enriched in the miR-492 region (Fig. 1D), and we next investigated whether the miR-492 genome locus was enriched in H3K27ac. Consistently, in response to miR-492 overexpression, ChIP–qPCR showed that the active enhancer marker H3K27ac was increased 2.7-fold when miR-492 was overexpressed compared to the empty vector (Fig. 2B). Compared to the control, p300 and pol II were also enriched 1.7-fold and 4-fold, respectively (Fig. 2C and 2D), which indicates that miR-492 is

related to enhancers, which may be a prerequisite for enhancer-associated miRNA function. In addition, we also verified that H3K27ac, p300 and pol II were increased when miR-492 was overexpressed by ChIP-PCR (Fig. S5A). We also observed by ChIP–qPCR that the enrichment of Pol II at the promoter of NR2C1/NDUFA12/TMCC3 was increased (Fig. 2F-H and S5B). Immunoblots demonstrated that the expression of H3K27ac and pol II was increased when miR-492 was overexpressed. Furthermore, Co-IP experiments indicated that interactions between H3K27ac and NR2C1 or Pol II were potentially increased in cells overexpressing miR-492 (Fig. 2K). Then, we examined whether the genome sequence containing the miR-492 locus can function as an enhancer. To test the potential enhancer activity of the miR-492 genome locus, a DNA fragment containing the miR-492 genome locus with H3K27ac enrichment was inserted into the pGL3 vector, named pGL3-Enhancer. We detected both the luciferase and Renilla activities in HEK293T cells with a Dual Luciferase Reporter Assay Kit (Promega) 48 h after transfection. As expected, the activity of the reporter gene increased after pGL3-Enhancer transfection compared to the control group with pGL3-Control vector transfection, demonstrating that the DNA fragment containing the miR-492 genome locus can serve as an enhancer (Fig. 2I).

We then used the CRISPR–Cas9 genome editing method to delete miR-492 in the HEK293T cell lines (Fig. 2A). GFP was observed in HEK293T cells under a fluorescence microscope after transfection with the HP180_px300_GFP empty vector (Fig. S4A) and sgRNA_HP180_px300_GFP vector (Fig. S4B). Then, GFP-labeled cell clones transfected with the GFP empty vector (Fig. S4C) and the sgRNA_HP180_px300_GFP vector (Fig. S4D) were sorted by FACS. After incubation, the mutant clones were identified by T7 endonuclease assays (Fig. S4E) and further verified by DNA sequencing (Fig. S4F). The increased level of miR-492 in the mutant clones was lower than that in HEK293T cells following transfection with premiR-492 (Fig. 2J). Additionally, the neighboring genes could

no longer be activated after the deletion of the enhancer region (Figure 2J). Overall, these results demonstrate that enhancer integrity may exert a critical influence by miR-492, which is also supported by the observations in the dual luciferase reporter assay.

To support the model that miR-492 targets its own chromatin regions, we performed AGO2 ChIP to analyze whether AGO was associated with this region. Our results showed that there was significantly more enrichment of AGO2 in the miR-492 locus in HEK293T cells overexpressing miR-492 than in the control group (Fig. 2E), supporting the idea that AGO2 can be recruited to the miR-492 genomic locus overlapping with the enhancer region and that miR-492 may recruit the AGO2 protein to enhance its positive regulatory processes.

miR-492, as an oncogenic miRNA, promotes cancer cell proliferation, migration and invasion

To determine the biological function of miR-492, CCK-8 and colony formation assays were performed to determine the proliferative capacity of PaCa cells. We observed that overexpression of miR-492 can drive the growth and proliferation of BxPC-3 and PANC-1 cells (Fig. 3A and 3B) transfected with premiR-492, while the knockdown of miR-492 decreased cell growth and proliferation in BxPC-3 and PANC-1 cells (Fig. 3A, 3C and S6B-C). In addition, we measured the metastatic capacity of PaCa cells using Transwell invasion and wound healing assays. We found that miR-492 successfully increased the migration distance of PaCa cells compared with the control in the wound healing assay (Fig. S6A and S6D-E). In contrast, inhibition of miR-492 reduced the migration distance in BxPC-3 and PANC-1 cells (Fig. S6A and S6D-E). Transwell invasion assays showed that overexpression of miR-492 significantly increased the number of migrated BxPC-3 and PANC-1 cells (Fig. 3D and S6F-G). In contrast, the miR-492 inhibitor reduced the number of migrated cells in

both PaCa cell lines (Fig. 3E and S6F-G). These results demonstrate that miR-492 overexpression significantly increased the invasive capacity of PaCa cells as an oncogenic miRNA.

To analyze the effect of miR-492 expression on PaCa patients, Kaplan–Meier Plotter was used for the survival analysis in the TCGA database containing 178 samples of PaCa patients (http://kmplot.com/analysis/). We observed that patients with high expression of miR-492 had a shorter overall survival than those with low expression of miR-492 (HR = 2.42, log-rank p = 0.001). These results indicate that miR-492 may predict a poor prognosis for patients with PaCa and be related to the EMT of pancreatic cancer (Fig. S7). To investigate whether miR-492 is involved in EMT, we observed by immunoblot analyses that the expression level of E-cadherin was decreased, whereas the expression levels of TGF-β, p-Smad3, SNAIL+SLUG, and vimentin were increased in BxPC-3 and PANC-1 (Fig. 3F) cells transfected with premiR-492, a result that was similar to miR-492 mimic transfection (Fig. 3F). miR-492 knockdown resulted in an increase in the expression level of E-cadherin, whereas TGF-β, p-Smad3, SNAIL+SLUG, and vimentin were decreased (Fig. 3F). Immunofluorescence analyses showed that overexpression of miR-492 reduced the protein expression of E-cadherin and increased the protein expression of vimentin in BxPC-3 and PANC-1 cells transfected with premiR-492 (Fig. S8), which is consistent with the immunoblot analyses of PaCa cells transfected with premiR-492 (Fig. 3F).

NR2C1 promotes cancer cell proliferation and induces EMT in PaCa cells

To further demonstrate that miR-492 participates in EMT by regulating its neighboring gene, we constructed an NR2C1 pEGFP vector. CCK-8 and colony formation assays showed that NR2C1 overexpression promoted cell proliferation in BxPC-3 and PANC-1 cells, while si-

NR2C1 had the opposite effect (Fig. 4A-C and S9B-C). Wound healing assays revealed that NR2C1 overexpression could facilitate the migrative capacity of PaCa cells, while si-NR2C1 impaired migrative capacity (Fig. S9A and S9D-E). We also found that the invasive capacity was strengthened when NR2C1 was overexpressed but impaired when si-NR2C1 was transfected into BxPC-3 and PANC-1 cells (Fig. 4D-E, S9F-G). We next observed that vimentin and SNAIL+SLUG were increased and E-cadherin was decreased when PaCa cells (BxPC-3 and PANC-1) were transfected with the NR2C1 pEGFP vector. In contrast, si-NR2C1 transfection had the opposite effect (Fig. 4F). Moreover, the knockdown of NR2C1 restored the miR-492-induced abnormal expression of EMT-associated genes in PaCa cells (BxPC-3 and PANC-1) in the rescue experiment. TGF-β, p-Smad3, SNAIL+SLUG, and vimentin expression in the premiR-492 + si-NR2C1 group was decreased, whereas E-cadherin was increased compared with that in the premiR-492 + si-NC group (Fig. 4G). Conversely, TGF-β, p-Smad3, SNAIL+SLUG, and vimentin expression in the miR-492 inhibitor + pEGFP-NR2C1 group was increased, whereas E-cadherin was decreased compared with that in the miR-492 inhibitor + pEGFP group (Fig. S10). To determine the role of NR2C1 in PaCa progression, GSEA_4.1.0 was used to perform functional enrichment analysis of the differentially expressed genes of PaCa in the TCGA database, which contained 178 samples of PaCa patients (http://www.gsea-msigdb.org/gsea/index.jsp). Interestingly, we found by gene functional enrichment analysis that NR2C1 was related to the EMT pathway (NES (normalized enrichment score) = -1.678, p = 0.014; Fig. S11). Thus, we hypothesize that miR-492 acts as an onco-miRNA in PaCa and can induce the epithelial-mesenchymal transition by regulating NR2C1 transcription, which plays a pivotal role in accelerating the pancreatic cancer process.

AntagomiR-492 represses PaCa tumorigenesis *in vivo*

To investigate whether the miR-492 inhibitor could repress PaCa cell growth *in vivo*, we constructed a xenograft tumor mouse model and administered intravenous injection of antagomiR-492. Subcutaneous tumor formation experiments revealed that injection of antagomir-492 had lower fluorescence intensity and tumor volumes than the control (Fig. 5A-5C), and miR-492 was knocked down 0.6-fold in the 5 nmol antagomiR-492 group (Fig. 5D). In addition, the weights of mice with xenograft tumors treated with antagomiR-492 were more stable than those of the control group (Fig. S12), which suggests that antagomir-492 could have a curative effect in mice and play a vital role in suppressing PaCa growth *in vivo*. qRT–PCR analysis also demonstrated that the expression of the NR2C1/NDUFA12/TMCC3 genes was downregulated. NR2C1, NDUFA12 and TMCC3 in the antagomir-492 group declined approximately 0.4-, 0.6- and 0.5-fold, respectively, at the RNA level in the 5 nmol antagomiR-492 group compared to the control (Fig. 5E). We further analyzed IFN-γ, TNFα, and TGF-β in the serum from xenograft tumor mice with and without intravenous injection of antagomiR-492. As shown in Fig. 5N-P, we found that the expression levels of IFN-γ (Fig. 5N) and TNFα (Fig. 5O) in the antagomiR-492 group were significantly higher than those in the control group ($p < 0.05$), indicating that antagomiR-492 can regulate the functions of some cytokines, such as IFN-γ and TNFα. In addition, we also verified that the expression levels of TGF-β in the serum of the antagomiR-492 group were lower than those in the control group (Fig. 5P), which suggests that miR-492 is associated with the TGF-β activation pathway.

Finally, using HE staining, we found that there was more vascular endothelium around the tumor and less collagenous fibrous tissues in the control group (Fig. 5F) than in the antagomiR-492 group (Fig. 5G). IHC analysis revealed significant decreases in the expression of NR2C1/NDUFA12/TMCC3 genes compared to the control (Fig. 5). NR2C1

was positively expressed in the nucleus (Fig. 5H-I), whereas NDUFA12 (Fig. 5J-K) and TMCC3 (Fig. 5L-M) were positively expressed in the cytoplasm. We further found apparent positive expression of E-cadherin in the cytoplasm and cell membrane of tumor cells in the antagomiR-492 group compared with weak expression in the cytoplasm and cell membrane of tumor cells in the control (Fig. S13A-B). On the other hand, vimentin was weakly positively expressed in the cytoplasm of tumor cells in the control group but almost absent in the cytoplasm of tumor cells in the antagomiR-492 group, although it was positively expressed in the stroma in the two groups (Fig. S13C-D). Finally, SNAIL was positively expressed in the cytoplasm and nucleus of tumor cells but not in the stroma in the two groups (Fig. S13E-F). These results indicate that antagomir-492 can evidently suppress the EMT process by downregulating the expression of the contiguous genes NR2C1, NDUFA12 and TMCC3 *in vivo*.

Discussion

Emerging studies have shown that abnormally expressed miRNAs are closely related to PaCa occurrence and development, which demonstrates that miRNAs play an important role in pancreatic carcinogenesis (32-34). miRNAs targeting KRAS and regulating its downstream genes have been identified in pancreatic cancer, and miR-96 and miR-217 can suppress KRAS activity and inhibit cancer cell migration and invasion of PaCa (35). miR-146a-5p and miRNA-141, as tumor suppressor miRNAs, can also reduce pancreatic cancer cell proliferation by targeting the 3'-untranslated region of TRAF6 (36) and MAP4K4 (37). Moreover, miR-146a-5p also sensitizes PaCa cancer cells to gemcitabine chemotherapy by regulating the TRAF6/NF-κB p65/P-gp axis (36). In this study, we showed that miR-492 was significantly upregulated in PaCa tumor tissues. We found that miR-492 can regulate

proliferation, invasion and migration in PaCa. We also demonstrated that miR-492 may be related to poor prognosis for patients with PaCa and lead to the EMT progression of pancreatic cancer.

Some distinct chromatin landmarks were identified as active promoters in human cells (24). H3K27ac is strongly associated with the promoters and enhancers of transcriptionally active genes (38-40). Additionally, the initiation of pol II transcription and p300/CBP are associated with enhancer activation (41-43). We further confirmed by ChIP–qPCR that the active enhancer marker H3K27ac was increased, which established H3K27ac, pol II and p300 as important enhancer markers for miR-492 that can distinguish between active and poised enhancer elements. Thus, we hypothesize that enhancer-associated miR-492 may be an oncogenic regulatory role of miR-492 via activation of the expression of the neighboring genes to impact the biological behavior of PaCa cells. In addition, using the UCSC genome browser, we also found that the neighboring genes of miR-492 were NR2C1, NDUFA12 and TMCC3 in an approximately 440 kb region, and H3K27ac was abundant in the miR-492 region, which led us to explore the role of miR-492 as an enhancer to activate adjacent gene expression. We observed that the expression of its neighboring gene NR2C1/NDUFA12/TMCC3 was also upregulated in PaCa tumor tissue, which indicated that the NamiRNA-enhanced gene activation network might contribute to providing new clues to pinpoint the regulatory function of miR-492 (31). We further used the adjacent miRNA (miR-331) of miR-492 as a control, which was without an H3K27ac enhancer marker. The expression levels of the neighboring NR2C1/NDUFA12/FGD6/VEZT genes of miR-331 were not significantly different from those of the control when miR-331 was overexpressed or knocked down. The above phenomenon suggests that miR-492 may be a specific regulator of NR2C1/NDUFA12/TMCC3 in the development and progression of PaCa, providing a potential target for future PaCa therapy.

miR-492 may influence PaCa progression via EMT, and to study this possibility, we observed that the expression level of E-cadherin was repressed, whereas vimentin was upregulated, in the two PaCa cell lines transfected with premiR-492 or miR-492 mimics. Furthermore, miR-492 was observed to induce EMT by activating NR2C1. A previous study showed that NR2C1 could regulate retinal progenitor cell transcription during retinal development (44) and was associated with stem cells in the developing olfactory epithelium (45) as a modulator of pluripotentiality during hominid evolution (46), which suggests that NR2C1 is involved in stem cell differentiation and EMT in cancer cells. At the same time, NR2C1/NDUFA12/TMCC3 expression was downregulated following transfection of the miR-492 inhibitor into PaCa cells. In support of this idea, we also showed that the miR-492 inhibitor repressed PaCa cell growth *in vivo* and downregulated the expression of NR2C1/NDUFA12/TMCC3. NR2C1 is a member of the steroid/thyroid hormone receptor superfamily (47), functions as a negative modulator to suppress androgen receptor action in prostate cancer (48), and has prognostic significance in HCC patients (49). TMCC3 is crucial for the maintenance of breast cancer stem cell (BCSC) features and interacts directly with AKT (50), which suggests that miR-492 may serve as a novel target for therapy directed against pancreatic stem cancer cells.

In summary, our results suggest that miR-492, as an enhancer trigger, can promote EMT in pancreatic cancer by activating the expression of NR2C1 and the TGF-β/Smad3 pathway. Our findings improve the understanding of PaCa-related NamiRNAs and support the development of miR-492-based therapies for pancreatic cancer.

Funding

This research was supported by a grant from the National Natural Science Foundation of China (81672383), a grant from Shanghai sailing program (19YF1441100), a grant from the Science and Technology Commission of Shanghai (20Y11900700), a grant (KY-GW-2020-09) from Shanghai Public Health Clinical Center and a grant from the Special Research Fund of Youan Medical Alliance for the Liver and Infectious Diseases (LM202020).

Acknowledgments

The authors want to thank all the staff in the Department of Laboratory Animal Science of Shanghai Public Health Clinical Center for their technical assistance.

Conflict of Interest Statement

The authors declare no potential conflicts of interest.

Abbreviations

3'UTRs：3' untranslated regions；ChIP：Chromatin immunoprecipitation； Co-IP：Coimmunoprecipitation；COX-2：cyclooxygenase-2； CRISPR–Cas 9：Clustered regularly interspaced short palindromic repeats and associated proteins 9；EMT：epithelial-mesenchymal transition；GJB4：gap junction beta-4 protein；IHC：Immunohistochemical ； KRT19： keratin 19; LATS2：large tumor suppressor kinase 2； NamiRNAs：nuclear

activating miRNAs； PaCa：Pancreatic cancer；PLAG1：pleomorphic adenoma gene 1；

sgRNAs：Single guide RNAs；

Data Availability Statements

The data underlying this article will be shared on reasonable request to the corresponding author.

References

1. Siegel, R.L., *et al.* (2016) Cancer statistics, 2016. *CA Cancer J Clin*, **66**, 7-30.
2. Sun, H., *et al.* (2014) Survival improvement in patients with pancreatic cancer by decade: a period analysis of the SEER database, 1981-2010. *Sci Rep*, **4**, 6747.
3. Renz, B.W., *et al.* (2017) Oligometastatic Disease in Pancreatic Cancer - How to Proceed? *Visc Med*, **33**, 36-41.
4. Hartwig, W., *et al.* (2013) Improvement of surgical results for pancreatic cancer. *Lancet Oncol*, **14**, e476-e485.
5. Zhou, P., *et al.* (2017) The epithelial to mesenchymal transition (EMT) and cancer stem cells: implication for treatment resistance in pancreatic cancer. *Mol Cancer*, **16**, 52.
6. Berindan-Neagoe, I., *et al.* (2014) MicroRNAome genome: a treasure for cancer diagnosis and therapy. *CA Cancer J Clin*, **64**, 311-36.
7. Rupaimoole, R., *et al.* (2017) MicroRNA therapeutics: towards a new era for the management of cancer and other diseases. *Nat Rev Drug Discov*, **16**, 203-222.
8. Wang, J., *et al.* (2014) Circulating microRNAs in Pancreatic Juice as Candidate Biomarkers of Pancreatic Cancer. *J Cancer*, **5**, 696-705.
9. von Frowein, J., *et al.* (2011) MicroRNA-492 is processed from the keratin 19 gene and up-regulated in metastatic hepatoblastoma. *Hepatology*, **53**, 833-42.
10. Shen, F., *et al.* (2015) MiR-492 contributes to cell proliferation and cell cycle of human breast cancer cells by suppressing SOX7 expression. *Tumour Biol*, **36**, 1913-21.
11. Jiang, J., *et al.* (2014) MicroRNA-492 expression promotes the progression of hepatic cancer by targeting PTEN. *Cancer Cell Int*, **14**, 95.
12. Gaedcke, J., *et al.* (2012) The rectal cancer microRNAome--microRNA expression in

rectal cancer and matched normal mucosa. *Clin Cancer Res*, **18**, 4919-30.

13. Wang, K., *et al.* (2019) miR-492 Promotes Cancer Progression by Targeting GJB4 and Is a Novel Biomarker for Bladder Cancer. *Onco Targets Ther*, **12**, 11453-11464.
14. Shi, L.P., *et al.* (2019) MiR-492 exerts tumor-promoting function in prostate cancer through repressing SOCS2 expression. *Eur Rev Med Pharmacol Sci*, **23**, 992-1001.
15. Wang, Z., *et al.* (2020) Effects of miR-492 on migration, invasion, EMT and prognosis in ovarian cancer by targeting SOX7. *J buon*, **25**, 797-804.
16. Wu, S., *et al.* (2020) miR-492 promotes chemoresistance to CDDP and metastasis by targeting inhibiting DNMT3B and induces stemness in gastric cancer. *Biosci Rep*, **40**.
17. von Frowein, J., *et al.* (2018) MiR-492 regulates metastatic properties of hepatoblastoma via CD44. *Liver Int*, **38**, 1280-1291.
18. Liu, M., *et al.* (2018) MicroRNA-492 overexpression involves in cell proliferation, migration, and radiotherapy response of cervical squamous cell carcinomas. *Mol Carcinog*, **57**, 32-43.
19. Sun, Z., *et al.* (2019) Inhibition of microRNA□492 attenuates cell proliferation and invasion in retinoblastoma via directly targeting LATS2. *Mol Med Rep*, **19**, 1965-1971.
20. Fabian, M.R., *et al.* (2010) Regulation of mRNA translation and stability by microRNAs. *Annu Rev Biochem*, **79**, 351-79.
21. Pasquinelli, A.E. (2012) MicroRNAs and their targets: recognition, regulation and an emerging reciprocal relationship. *Nat Rev Genet*, **13**, 271-82.
22. Bartel, D.P. (2004) MicroRNAs: genomics, biogenesis, mechanism, and function. *Cell*, **116**, 281-97.
23. Matsui, M., *et al.* (2013) Promoter RNA links transcriptional regulation of inflammatory pathway genes. *Nucleic Acids Res*, **41**, 10086-109.

24. Majid, S., *et al.* (2010) MicroRNA-205-directed transcriptional activation of tumor suppressor genes in prostate cancer. *Cancer*, **116**, 5637-49.

25. Xiao, M., *et al.* (2017) MicroRNAs activate gene transcription epigenetically as an enhancer trigger. *RNA Biol*, **14**, 1326-1334.

26. Huang, V., *et al.* (2012) Upregulation of Cyclin B1 by miRNA and its implications in cancer. *Nucleic Acids Res*, **40**, 1695-707.

27. Janowski, B.A., *et al.* (2007) Activating gene expression in mammalian cells with promoter-targeted duplex RNAs. *Nat Chem Biol*, **3**, 166-73.

28. Yue, X., *et al.* (2010) Transcriptional regulation by small RNAs at sequences downstream from 3' gene termini. *Nat Chem Biol*, **6**, 621-9.

29. Smith, E., *et al.* (2014) Enhancer biology and enhanceropathies. *Nat Struct Mol Biol*, **21**, 210-9.

30. Liang, Y., *et al.* (2021) Reactivation of tumour suppressor in breast cancer by enhancer switching through NamiRNA network. *Nucleic Acids Res*, **49**, 8556-8572.

31. Liang, Y., *et al.* (2019) An epigenetic perspective on tumorigenesis: Loss of cell identity, enhancer switching, and NamiRNA network. *Semin Cancer Biol*, **57**, 1-9.

32. Xu, B., *et al.* (2018) Expression of miRNA-143 in Pancreatic Cancer and Its Clinical Significance. *Cancer Biother Radiopharm*, **33**, 373-379.

33. Fang, Y., *et al.* (2019) Exosomal miRNA-106b from cancer-associated fibroblast promotes gemcitabine resistance in pancreatic cancer. *Exp Cell Res*, **383**, 111543.

34. Chen, Y., *et al.* (2019) MicroRNA hsa-miR-623 directly suppresses MMP1 and attenuates IL-8-induced metastasis in pancreatic cancer. *Int J Oncol*, **55**, 142-156.

35. Tesfaye, A.A., *et al.* (2019) miRNA and Gene Expression in Pancreatic Ductal Adenocarcinoma. *Am J Pathol*, **189**, 58-70.

36. Meng, Q., *et al.* (2020) A miR-146a-5p/TRAF6/NF-kB p65 axis regulates pancreatic

cancer chemoresistance: functional validation and clinical significance. *Theranostics*, **10**, 3967-3979.

37. Zhao, G., *et al.* (2013) miRNA-141, downregulated in pancreatic cancer, inhibits cell proliferation and invasion by directly targeting MAP4K4. *Mol Cancer Ther*, **12**, 2569-80.

38. Ernst, J., *et al.* (2011) Mapping and analysis of chromatin state dynamics in nine human cell types. *Nature*, **473**, 43-9.

39. Whyte, W.A., *et al.* (2013) Master transcription factors and mediator establish super-enhancers at key cell identity genes. *Cell*, **153**, 307-19.

40. Heintzman, N.D., *et al.* (2007) Distinct and predictive chromatin signatures of transcriptional promoters and enhancers in the human genome. *Nat Genet*, **39**, 311-8.

41. De Santa, F., *et al.* (2010) A large fraction of extragenic RNA pol II transcription sites overlap enhancers. *PLoS Biol*, **8**, e1000384.

42. Kim, T.K., *et al.* (2010) Widespread transcription at neuronal activity-regulated enhancers. *Nature*, **465**, 182-7.

43. Raisner, R., *et al.* (2018) Enhancer Activity Requires CBP/P300 Bromodomain-Dependent Histone H3K27 Acetylation. *Cell Rep*, **24**, 1722-1729.

44. Olivares, A.M., *et al.* (2017) The nuclear hormone receptor gene Nr2c1 (Tr2) is a critical regulator of early retina cell patterning. *Dev Biol*, **429**, 343-355.

45. Baker, J.L., *et al.* (2016) Testicular receptor 2, Nr2c1, is associated with stem cells in the developing olfactory epithelium and other cranial sensory and skeletal structures. *Gene Expr Patterns*, **20**, 71-9.

46. Baker, J.L., *et al.* (2016) Functional Divergence of the Nuclear Receptor NR2C1 as a Modulator of Pluripotentiality During Hominid Evolution. *Genetics*, **203**, 905-22.

47. Lin, D.L., *et al.* (2000) Identification of an essential cis-acting element (TR2-PACE)

in the 5' promoter of human TR2 orphan receptor gene. *Endocrine*, **12**, 89-97.

48. Mu, X., *et al.* (2003) TR2 orphan receptor functions as negative modulator for androgen receptor in prostate cancer cells PC-3. *Prostate*, **57**, 129-33.

49. Sun, G., *et al.* (2021) Human nuclear receptors (NRs) genes have prognostic significance in hepatocellular carcinoma patients. *World J Surg Oncol*, **19**, 137.

50. Wang, Y.H., *et al.* (2021) Transmembrane and coiled-coil domain family 3 (TMCC3) regulates breast cancer stem cell and AKT activation. *Oncogene*, **40**, 2858-2871.

Figure legends

Figure 1: miR-492 activates neighboring genes in pancreatic cancer. A-B) miR-492; E, H) NR2C1; F, I) NDUFA12; G, J) TMCC3; C) Fluorescence in situ hybridization of miR-492 in BxPC-3 and PANC-1 cells; D) miR-492 region in the UCSC genome browser; K-M) Real-time PCR (qRT–PCR) analysis of miR-492, NR2C1, NDUFA12, and TMCC3 mRNA expression when miR-492 was overexpressed in BxPC-3 (K) and PANC-1 cells (L) and knocked down in pancreatic cancer cells (M); N-O) Western blot analysis of NR2C1, NDUFA12, and TMCC3 mRNA expression when miR-492 was overexpressed and knocked down in BxPC-3 (N) and PANC-1 cells (O); P, Q) NR2C1, NDUFA12, and TMCC3 mRNA expression in the nucleus and cytoplasm of BxPC-3 (P) or PANC-1 cells (Q) when miR-492 was overexpressed and knocked down in pancreatic cancer cells. Data represent the mean ± SD of 3 separate experiments. *$p < 0.05$, **$p < 0.01$, ***$p < 0.001$ by Student's t test.

Figure 2: sgRNA: Cas9-mediated miR-492 mutations and ChIP analysis in the 293T cell line. A) Schematic diagram of the sgRNA target sites at the miR-492 locus. ChIP analysis of H3K27ac (B), p300 (C), pol II (D) and AGO2 (E) when miR-492 was overexpressed; F-H); ChIP analysis of Pol II at the promoter of NR2C1 (F), NDUFA12 (G) and TMCC3 (H) when miR-492 was overexpressed; I) miR-492 genome locus acts as an enhancer as shown by a Dual Luciferase Reporter Assay; J) qRT–PCR analysis of rescue experiments; K) H3K27ac-related immunoprecipitation was used to assess the levels of H3K27ac and NR2C1. Data represent the mean ± SD of 3 separate experiments. *$p < 0.05$, **$p < 0.01$, ***$p < 0.001$ by Student's t test.

Figure 3: miR-492 overexpression promotes cell proliferation and invasion in pancreatic cancer. A) CCK-8 assays were performed to determine the viability of BxPC-3 and PANC-1 transfected with premiR-492 (A i and A ii) and miR-492 inhibitor(A iii and A iv); B-C) colony formation assays were used to detect the proliferation of pancreatic cancer cells transfected with premiR-492 (B) and miR-492 inhibitor (C); D-E) Transwell assays were used to detect the invasion ability of pancreatic cancer cells transfected with premiR-492 (D) or miR-492 inhibitor (E); F) Western blot analysis of EMT indicators when miR-492 was overexpressed or knocked down in BxPC-3 and PANC-1 cells. Data represent the mean ± SD of 3 separate experiments. *$p < 0.05$, **$p < 0.01$, ***$p < 0.001$ by Student's t test.

Figure 4: NR2C1 overexpression promotes cell proliferation and invasion in pancreatic cancer. A) CCK-8 assays were performed to determine the viability of BxPC-3 and PANC-1 transfected with pEGFP-NR2C1 (A i and A ii) and si-NR2C1 (A iii and A iv); B-C) colony formation assays were used to detect the proliferation of pancreatic cancer cells transfected with pEGFP-NR2C1 (B) and si-NR2C1 (C); D-E) Transwell assays were used to detect the invasion ability of pancreatic cancer cells transfected with pEGFP-NR2C1 (D) or si-NR2C1 (E); F) Western blot analysis of EMT indicators when NR2C1 was overexpressed or knocked down in BxPC-3 and PANC-1 cells; G) Western blot analysis of EMT indicators in rescue experiments in BxPC-3 and PANC-1 cells. Data represent the mean ± SD of 3 separate experiments. *$p < 0.05$, **$p < 0.01$, ***$p < 0.001$ by Student's t test.

Figure 5: A**ntagomiR-492 inhibits cell growth and proliferation *in vivo***. A, C) Fluorescence intensity imaging in mice; B) The volume of xenograft tumor; D) qRT–PCR analysis of miR-492 mRNA level in xenograft tumor mice with and without the intravenous injection of antagomiR-492; E) qRT–PCR analysis of NR2C1, NDUFA12, and TMCC3 mRNA expression levels in xenograft tumor mice with and without the intravenous injection of antagomiR-492; I-X) HE staining and IHC analyses of mouse xenograft tumor tissue samples from the intravenous injection of control (F, H, J and L) or antagomiR-492 (G, I, K and M); HE staining (F and G: red arrow refers to tumor cells, yellow arrow refers to vascular endothelium around the tumor, and black arrows indicate the collagen fibrous tissue); Immunohistochemical analysis (F-M) of NR2C1, NDUFA12 and TMCC3 protein expression in mouse tumor tissue samples stained with anti-NR2C1 (H and I), anti-NDUFA12 (J and K), and anti-TMCC3 antibodies (L and M). The red arrows indicate positive, the orange arrows indicate weakly positive expression, and the black arrows indicate negative expression in tumor cells, IHC × 400). N-P) IFN-γ (N), TNF-α (O) and TGF-β (P) in the serum from xenograft tumor mice with and without intravenous injection of antagomiR-492 were assayed using ELISA. Data represent the mean ± SD of 3 separate experiments. *$p < 0.05$, **$p < 0.01$, ***$p < 0.001$ by Student's t test.

Figure 1

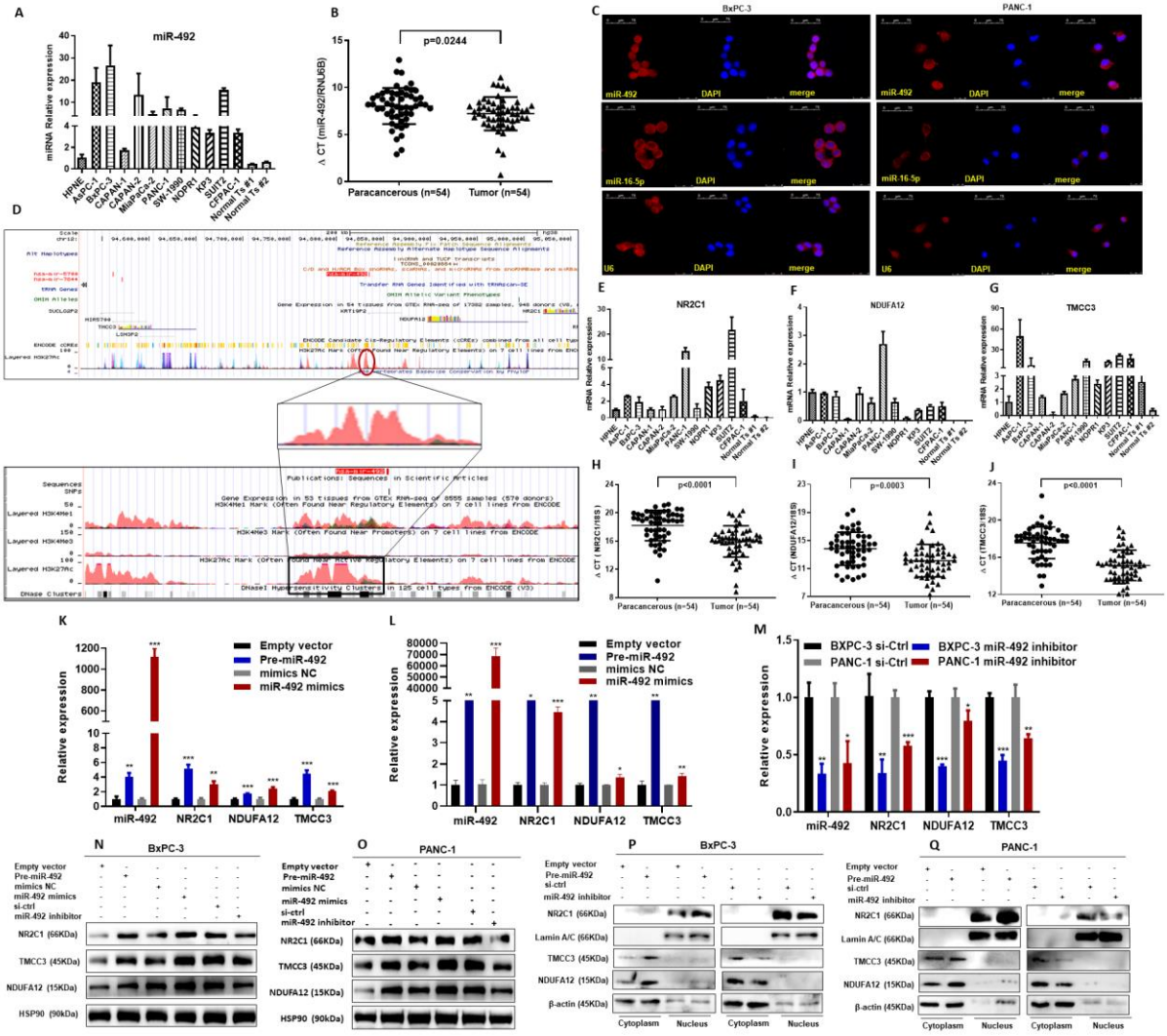

Figure 2

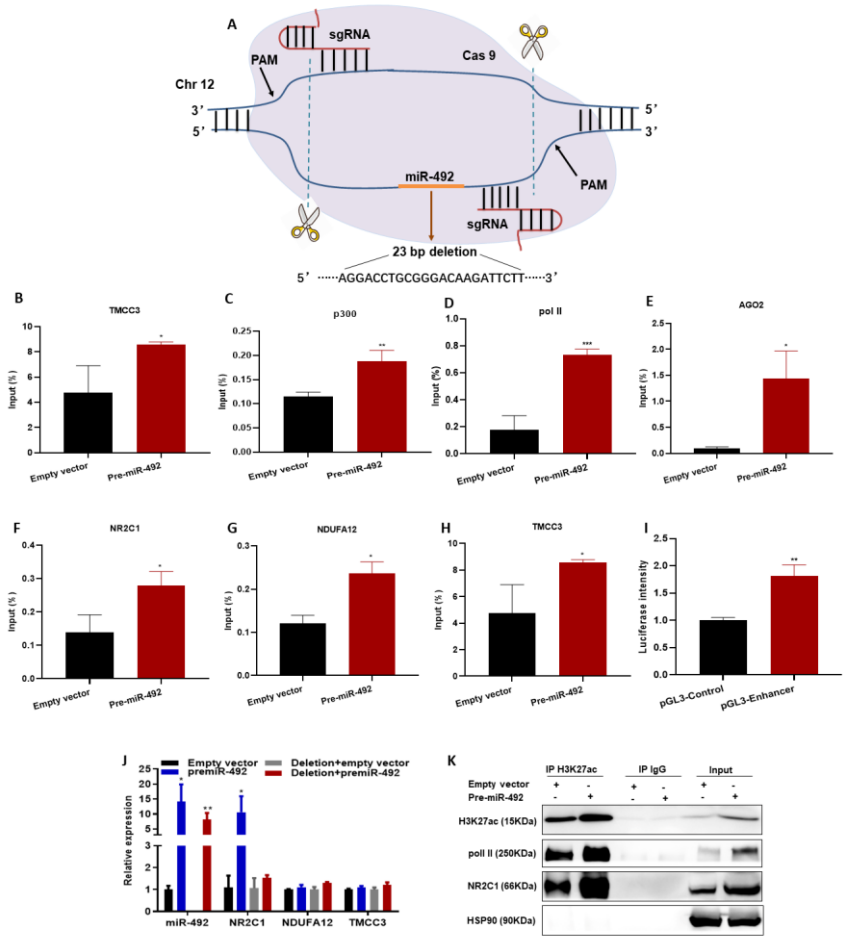

Figure 3

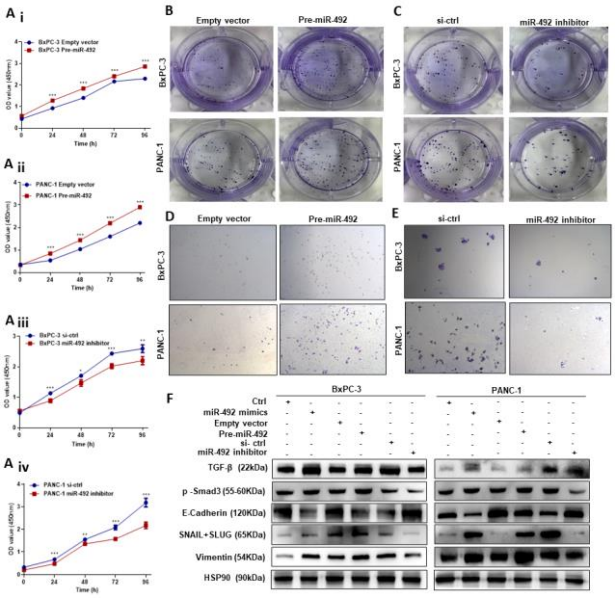

Figure 4

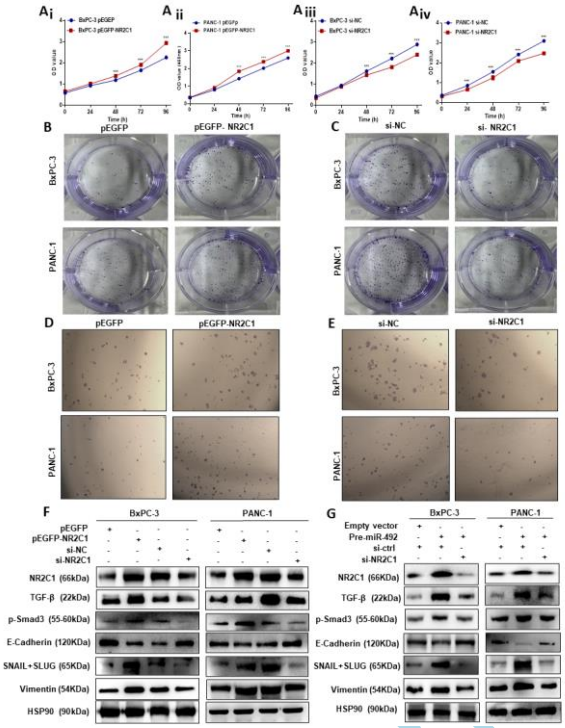

Figure 5